The electronic structure of $M_xMo_6Se_{8-\delta}$ Chevrel phases with defects

LETTER TO THE EDITOR

The electronic structure of $M_x Mo_6 Se_{8-\delta}$ Chevrel phases with defects

J Tobola[1,2]**, P Pecheur**[1,4]**, H Scherrer**[1]**, S Kaprzyk**[2]**, Y Ohta**[3] **and Y Matsumura**[3]

[1] Laboratoire de Physique des Materiaux, Ecole des Mines, Parc de Saurupt, 54042 Nancy Cedex, France
[2] Faculty of Physics and Nuclear Techniques, AGH University of Science and Technology, Aleja Mickiewicza 30, 30-059 Cracow, Poland
[3] Japan Ultra-High Temperature Materials Research Institute, 573-3 Okiube, Ube, Yamaguchi, 755-0001, Japan

E-mail: pecheur@mines.inpl-nancy.fr

Abstract
The electronic structure of defected $M_x Mo_6 Se_{8-\delta}$ Chevrel phases (M = Ti, Sn and vacancy) is investigated with the KKR–CPA method. In all cases presented the Se vacancy does appear to behave as a double donor, filling some of the holes below the gap. From the computed densities of states the stability of the defects in these compounds can be understood through the presence of an energy gap near the Fermi level. Then it seems energetically favourable to fill the bonding holes at the valence band edge, which may tentatively explain why $x > 1$ in $Sn_x Mo_6 Se_{7.5}$ ($x \approx 1.2$), and $x < 1$ in $Ti_x Mo_6 Se_{7.5}$ ($x \leqslant 0.8$). The low DOS at E_F corresponds well to the semi-metallic properties of the $Ti_{0.8} Mo_6 Se_{7.5}$ alloy, previously observed in resistivity experiments.

1. Introduction

Chevrel phases with the general formula $M_x Mo_6 X_8$ (M = alkaline, alkaline earth, transition metal, rare earth or actinide and X = S, Se or Te) have been known since the early 1970s [1]. Initially, these compounds attracted special attention due to their unusual crystal structure, rare earth magnetism [2], superconductivity [3] and intriguing electronic structure behaviour [4, 5]. Recently, these Chevrel phases have been considered as promising thermoelectric materials [6–8], since some of the compounds possess both a narrow band gap and a low thermal conductivity. Indeed, semiconducting properties and rather high thermopower have been experimentally detected in $Ti_x Mo_6 Se_8$ and $Zn_x Mo_6 Se_8$ [9].

[4] Author to whom any correspondence should be addressed.

Chevrel phases mostly crystallize in a rhombohedral symmetry (space group $R\bar{3}$) but some of them present a triclinic deformation (space group $P\bar{1}$). The crystal structure of these compounds can be viewed as a stacking of slightly distorted Mo_6X_8 cubes (one Mo_6X_8 block per unit cell), where the Se atoms are placed near the corners while the Mo atoms remain almost in the face-centred positions. The Mo_6X_8 pseudo-cube is rotated around the common axis (a body diagonal and a rhombohedral one) by an angle $\approx 27°$ (see [3]). As the two Se atoms located on the 3-fold axis are more distanced, with respect to the cubic positions, there are two inequivalent sites of selenium: 2(c) and 6(f). Such a particular arrangement of the Mo_6X_8 units in the rhombohedral cell leaves a certain number of cavities. The largest one is situated at the origin of the unit cell and is often filled by large atoms (Sn or Pb). Smaller atoms usually occupy smaller cavities distributed on the 6(f) positions.

Another remarkable feature of these materials comes from the existence of a gap in the electronic spectrum between bonding and anti-bonding states, formed mainly from p-Se and d-Mo states. The band gap position corresponds to 36 completed bands, which may accommodate 72 electrons, if the lower lying and well separated s states of Se are not taken into account. So, the physical properties of the $M_xMo_6Se_8$ phases should mainly depend on the number of valence electrons in the cluster. In Mo_6X_8, for example, the p–d block of bands is filled up to 34 bands due to $6Mo \times 6 + 8Se \times 4 = 68$ valence electrons and the system has 4 holes below the gap. A similar analysis in $SnMo_6Se_8$, namely $6Mo \times 6 + 8Se \times 4 + 1Sn \times 2 = 70$, allows describing this compound as a 2-hole system, taking into account the s band of Sn which appears just below the p–d Mo_6Se_8 valence band (Sn is then in the Sn^{2+} state). Consequently, in the stoichiometric $TiMo_6Se_8$ and $Zn_2Mo_6Se_8$ (the filled d shell of Zn was found below the p-Se and d-Mo valence states), the 36 bands are completed and the Fermi level is expected to fall into the gap [6, 8] (note that in the Zn case, there is not a separate Zn s band).

Chevrel phases often exhibit defects not only in the M lattice but also in the chalcogen network. Such a crystallographic behaviour has been observed quite regularly in several studies, where the sample stoichiometry was precisely determined. For instance, in the work of Roche [9] and Ushida et al [10], $Ti_{0.88}Mo_6Se_{7.5}$ and $Zn_{0.3}Ti_{0.5}Mo_6Se_{7.5}$ were obtained in place of $TiMo_6Se_8$ and $ZnTiMo_6Se_8$. In the recent photoemission study [11], $Mo_6Se_{8-\delta}$ and $Sn_xMo_6Se_{8-\delta}$ (with $\delta \approx 0.5$) were investigated and it was assumed that the Se vacancy was a double donor. Indeed, this occurs if the repulsive potential of the vacancy is sufficient to expel from the valence band the s and p levels of the removed Se. Since these levels were filled with 8 electrons and since only 6 electrons are removed with a neutral Se atom, the Se vacancy gives 2 electrons to the valence band. Simple tight binding calculations [12, 13] have already indicated that the Se and Te isolated vacancies are double donors in PbSe and Bi_2Te_3.

Such behaviour prompted us to perform a theoretical study of the effect of the Se deficiency on the electronic structure of $SnMo_6Se_{8-\delta}$ and $TiMo_6Se_{8-\delta}$. We used the KKR–CPA method which can cope with finite concentrations of vacancies.

2. Electronic structure calculations

The electronic structure computations on the disordered $M_xMo_6X_{8-\delta}$ were performed using the charge self-consistent Korringa–Kohn–Rostoker method with the coherent potential approximation (CPA). The crystal potential of muffin-tin form was constructed within the LDA framework, using the von Barth–Hedin [14] formula for the exchange–correlation part. The Fermi energy was determined precisely (≈ 0.1 mRyd) via the generalized Lloyd formula [15], using an elliptic contour in the complex energy plane. The KKR–CPA Green function was computed on a 75 special k-point mesh in the irreducible part of the Brillouin zone. The self-consistency cycles were repeated until input–output differences of the potentials and charges
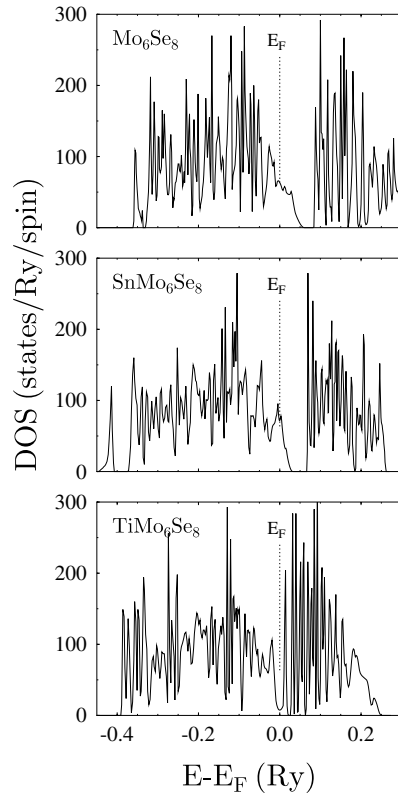
Figure 1. KKR DOS in undefected MMo_6Se_8 (M = vacancy, Sn and Ti) Chevrel phases. The Fermi level (E_F) is at zero.

inside the muffin-tin spheres were of order 1 mRyd and 10^{-3} e, respectively. KKR calculations performed for perfect crystals with a maximum angular momentum $l_{max} = 3$ have shown only slight differences on density of states with results obtained with $l_{max} = 2$ (especially in the vicinity of the Fermi level). So, for the more time-consuming KKR–CPA computations we used $l_{max} = 2$. For the final potentials the total density of states (DOS), site-decomposed DOS and l-decomposed partial DOS were computed using a tetrahedral k-space integration technique. More details concerning the KKR–CPA methodology used in our computations can be found in [16].

In our computations a cubic approximation of the real $M_x Mo_6Se_{8-\delta}$ crystal structure was used. Atoms were placed either in rhombohedral or in triclinic crystallographic positions but with the assumption that $\alpha_R = 90°$ and $\alpha = \beta = \gamma = 90°$, respectively. Thus, Mo atoms occupied 6(f) positions $[x, y, z]$, while Se entered both 6(f) $[x, y, z]$ and 2(e) $[x, x, x]$ sites. The big cation (Sn) resided on the 1(a) site $[0, 0, 0]$. Note that the rhombohedral deformation of the $SnMo_6Se_{8-\delta}$ cell is small ($\alpha_R = 89.6°$), which may justify the use of the cubic symmetry in our electronic structure calculations.

The lattice constants of $Mo_6Se_{8-\delta}$, $SnMo_6Se_{8-\delta}$ and $TiMo_6Se_{8-\delta}$ were taken as 6.658, 6.754 and 6.658 Å. Both unit cell and positional parameters were taken from experimental refinements [3]. Empty spheres were added to increase the packing ratio, which in the Chevrel phases is relatively low ($\approx 40\%$). Finally, the effect of a vacancy was investigated on the 2(e) site of Se atoms.
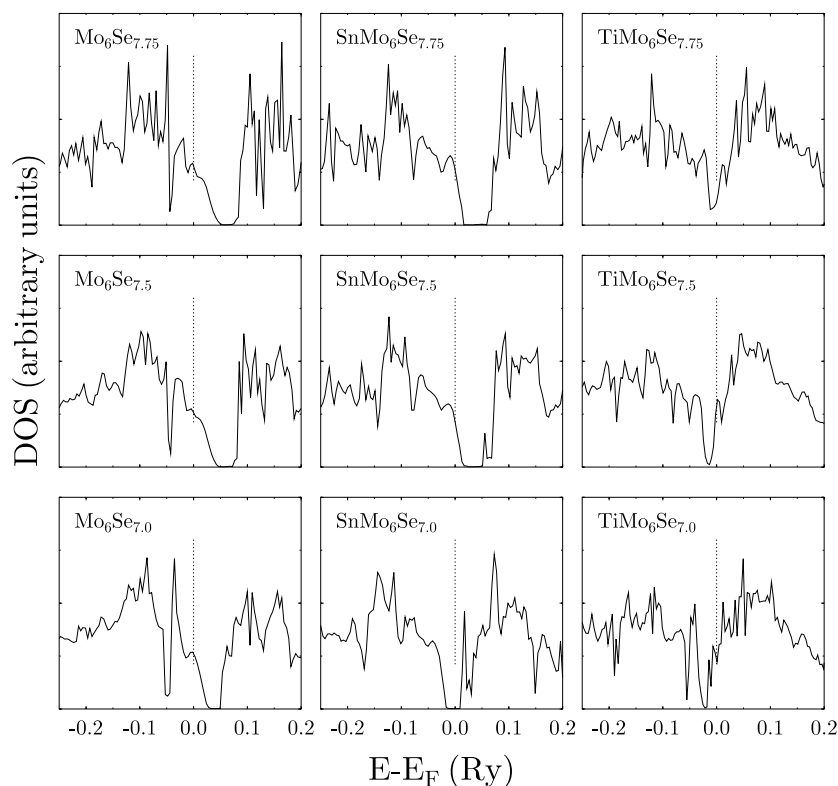
Figure 2. The evolution of the KKR–CPA DOS versus the concentration of defects (δ) in MMo$_6$Se$_{8-\delta}$ (M = vacancy, Sn and Ti) Chevrel phases. The Fermi level (E_F) is at zero.

On the whole we expect that even if the cubic approximation may somewhat modify the dispersion curves with respect to the rhombohedral or triclinic deformations of the real Chevrel phases, the influence on the DOS will be rather weak and should not invalidate the results of the vacancy effect computations.

3. Results and discussion

The total DOS of pure Mo$_6$Se$_8$, SnMo$_6$Se$_8$ and TiMo$_6$Se$_8$ calculated from the KKR method are presented in figure 1. At first sight we observe that in both Mo$_6$Se$_8$ and SnMo$_6$Se$_8$ there is an energy gap in the electronic structure above the Fermi level, which remains in agreement with previous band structure calculations [4, 5, 7, 11]. The valence states formed essentially from p-Se and d-Mo states indeed contain 36 bands. So, Mo$_6$Se$_8$ and SnMo$_6$Se$_8$ are 4-hole and 2-hole compounds, respectively, as found previously. In TiMo$_6$Se$_8$, E_F lies in a deep DOS minimum (figure 1) rather than in an energy gap. Note, however, that from the dispersion curves $E(\mathbf{k})$ calculated in TiMo$_6$Se$_8$ a gap was detected along a few high-symmetry directions in the Brillouin zone. The band structure calculations in the Zn$_2$Mo$_6$Se$_8$ system resulted in an energy gap of the order of 0.2 eV [17].

Figure 2 shows the effect of an Se vacancy on the electronic structure. The Fermi level shifts to upper lying states when the vacancy concentration increases and then approaches the gap.

Mo$_6$Se$_{7.5}$ has one electron more in respect to the undefected compound and there are three holes between the Fermi level and the energy gap. In SnMo$_6$Se$_{7.5}$, one hole appears between

the gap and E_F instead of two holes in the perfect $SnMo_6Se_8$. In the extremely defected $SnMo_6Se_{7.0}$, E_F should fall into the energy gap. In $Ti_xMo_6Se_{8-\delta}$ the Se vacancy defects tend to expel the Fermi level above the gap in a high DOS peak, which corresponds to a metallic state. Simultaneously, the DOS valley between valence and conduction states becomes deeper with increase of vacancy concentration.

Summarising, in all cases presented the Se vacancy does appear to behave as a double donor, filling some of the holes below the gap.

It can be noted that the experimental samples are also non-stoichiometric with respect to the interstitials: $Sn_{1.2}Mo_6Se_{7.5}$ has an excess of Sn and $Ti_{0.5}Mo_6Se_{7.5}$ exhibits a deficiency in Ti. This can be understood if the stability of the compounds is related to the gap. It should then be energetically favourable to fill the bonding holes at the valence band edge. In $SnMo_6Se_{7.5}$ one hole remains allowing an excess up to 0.5 Sn. On the contrary, in $Ti_xMo_6Se_{7.5}$, the valence states are full, which limits the Ti concentration to values lower than 0.75 (at least in samples with 0.5 Se vacancy). This is also in line with the semimetallic properties of the $Ti_{0.8}Mo_6Se_{7.5}$ system as revealed from the resistivity measurements [9].

References

[1] Chevrel R and Sergent M 1971 *J. Solid State Chem.* **3** 515
[2] Yvon K 1979 *Current Topics in Material Science* vol 3, ed E Kaldis (Amsterdam: North-Holland) p 53
[3] Fisher O and Maple M B (ed) 1982 *Superconductivity in Ternary Compounds I* (*Springer Topics in Current Physics* vol 32) (Berlin: Springer)
[4] Andsersen O K, Klose W and Nohl H 1978 *Phys. Rev.* B **17** 1209
[5] Freeman A J and Jarlborg T 1982 *Superconductivity in Ternary Compounds I* (*Springer Topics in Current Physics* vol 32) ed O Fisher and M B Maple (Berlin: Springer) p 165
[6] Roche C, Pecheur P, Toussaint G, Jenny A, Scherrer H and Scherrer S 1998 *J. Phys.: Condens. Matter* **10** L333
[7] Nunes R W, Mazin I I and Singh D J 1999 *Phys. Rev.* B **59** 7969
[8] Roche C, Chevrel R, Jenny A, Pecheur P, Scherrer H and Scherrer S 1999 *Phys. Rev.* B **60** 16442
[9] Roche C 2000 *PhD Thesis* INPL Nancy
[10] Uchida H, Roche C, Scherrer H, Tanahashi H, Kasama H, Matsuura M and Matsubara K 2000 *ICT2000: Proc. 19th Int. Conf. on Thermoelectrics (Cardiff, 2000)* p 143
[11] Kobayashi K, Fujimori A, Ohtani T, Gasgupta I, Jepsen O and Andersen O K 2001 *Phys. Rev.* B **63** 195109
[12] Parada N J and Pratt G W 1969 *Phys. Rev. Lett.* **22** 180
[13] Pecheur P and Toussaint G 1994 *J. Phys. Chem. Solids* **55** 327
[14] von Barth U and Hedin L 1972 *J. Phys. C: Solid State Phys.* C **5** 1629
[15] Kaprzyk S and Bansil A 1990 *Phys. Rev.* B **42** 7358
[16] Bansil A, Kaprzyk S, Mijnarends P E and Tobola J 1999 *Phys. Rev.* B **60** 13396
[17] Roche C, Chevrel R, Tobola J, Pecheur P, Scherrer H and Scherrer S 2000 *ICT99: Proc. 18th Int. Conf. on Thermoelectrics (Baltimore, MD, 2000)* p 610